Title: Examining the evidence for Superdense Exposed Cores in Extrasolar Systems.

Authors: Bates-Tarasewicz, Haley[1*]

Affiliations:

[1]Department of Aerospace Engineering and Earth Atmospheric and Planetary Science, Massachusetts Institute of Technology, Cambridge, MA 02139

*Corresponding Author. Email: hbates@mit.edu

Abstract:

Exoplanets provide a unique opportunity to view the edge cases and extremes of planetary formation, composition, and evolution, and with more extra-solar planets being confirmed each year, never has it been more possible to attempt to understand the hidden mechanisms behind planetary formation. Planetary cores have been of notable interest recently as they give insight into the history of planets as well as the properties of the protoplanetary disk and conditions under which the planet formed. This study examines the evidence for superdense exposed planetary cores and finds 24 new candidates, 16 more than previous work, and finds them loosely consistent with a proposed "Fossilized Core Theory" of formation.

Main Text:

Every year, more and more planets in other solar systems are discovered and confirmed. These exoplanets are a unique opportunity to understand the intricacies of planetary formation and evolution by shedding light on some of the more exotic outcomes, the edge cases and extremes. Planetary interiors are of specific interest as they help explain the mechanisms of planetary formation during the earliest stages of

the solar system, the composition of the planet, and its long-term evolution. Broadly, there are two ways in which planets can lose their outer mass, leaving their cores exposed.

The first is through powerful impacts in the early solar system (*1*). Planetesimals are thought to violently collide with one another, either sticking togther and growing in mass, or fracturing and splitting if the impact is strong enough (*2*). Under extreme cases, the energy of the impact can strip one or both of the planets of their outer layers, leaving only the dense, differentiated iron core (*1, 3*). This process is best understood for rocky, terrestrial planets. Examples in our own solar system include 16-Psyche, a massive metallic body in the asteroid belt (*3*).

The second mechanism in which cores can become exposed is through the hydrodynamic escape of a gas or ice giants (*4-7*). Gas or ice giants which have lost their massive envelopes, leaving behind only the dense rocky cores, are known as Chthonian planets (*6*). This work will be mostly focusing on Chthonian planets.

The composition of a planet can be estimated by comparing its measured radii to that of a hypothetical sphere of a proposed composition of the same mass (*8-11*), which can be modeled by assuming a spherical planet and using the mass of a shell of a given radius, hydrostatic equilibrium, and an equation of state (EOS) that relates density, pressure, and temperature for a given material in thermodynamic equilibrium (*8, 9*). However, this form of estimating bulk composition is highly degenerate -- by mass-radius data alone, there's no way to, for example, reliably differentiate a planet made entirely of water from one made of iron with a thick hydrogen atmosphere (*8*). Luckily, because exposed exoplanet cores are thought to be very dense and made mostly of iron (*1, 3, 6, 7*), findings in this vein have higher certainty, as iron is the heaviest cosmically abundant material (*12*) and planets are not expected to be

significantly denser than iron. However, as is discussed later, other exceptional circumstances can still lead to uncertainties in composition if the body is, for example, compressed.

In many cases, empirical data is used to derive specific EOSs for each material of interest (*8, 9*) and mass-radius curves are found from those measurements. However, the EOS for most materials share a very similar form, and so a generic mass-radius relationship can be found from a modified polytropic equation of state that incorporates the low compressibility of materials at low pressures (*8*). The generic, dimensionless mass-radius relationship for an iron body found by Seager et al. (*8*) and used in this study is:

$$log_{10}(R_s) = k1 + \tfrac{1}{3} \cdot log_{10}(M_s) - k2 \cdot M_s^{k3} \quad (1)$$

Where

$$R_s = \frac{R}{R_1}$$

$$M_s = \frac{M}{M_1}$$

Where the constants $R_s,\ M_s,\ k1,\ k2,$ and $k3$ vary depending on material (*8*). For iron, these values are $R_1 = 2.52R_{Earth},\ M_1 = 5.8M_{Earth},\ k1 = -0.20945,\ k2 = 0.0804,$ and $k3 = 0.394$ (*8*).

All data used was from the Extrasolar Planets Encyclopaedia (see exoplanet.eu) (*13*), which has published data for 3715 confirmed exoplanets. Discarding those that were missing experimentally measured values for mass and/or radius left 628 analyzable candidates. The mass-radius relationship given above in equation 1 is only reasonably accurate for up to $\sim 100M_{Earth}$ (*8*), so only planets less massive than this cutoff mass were considered, leaving 236 planets as potential candidates. Figure 1 presents the preliminary mass-radius data.

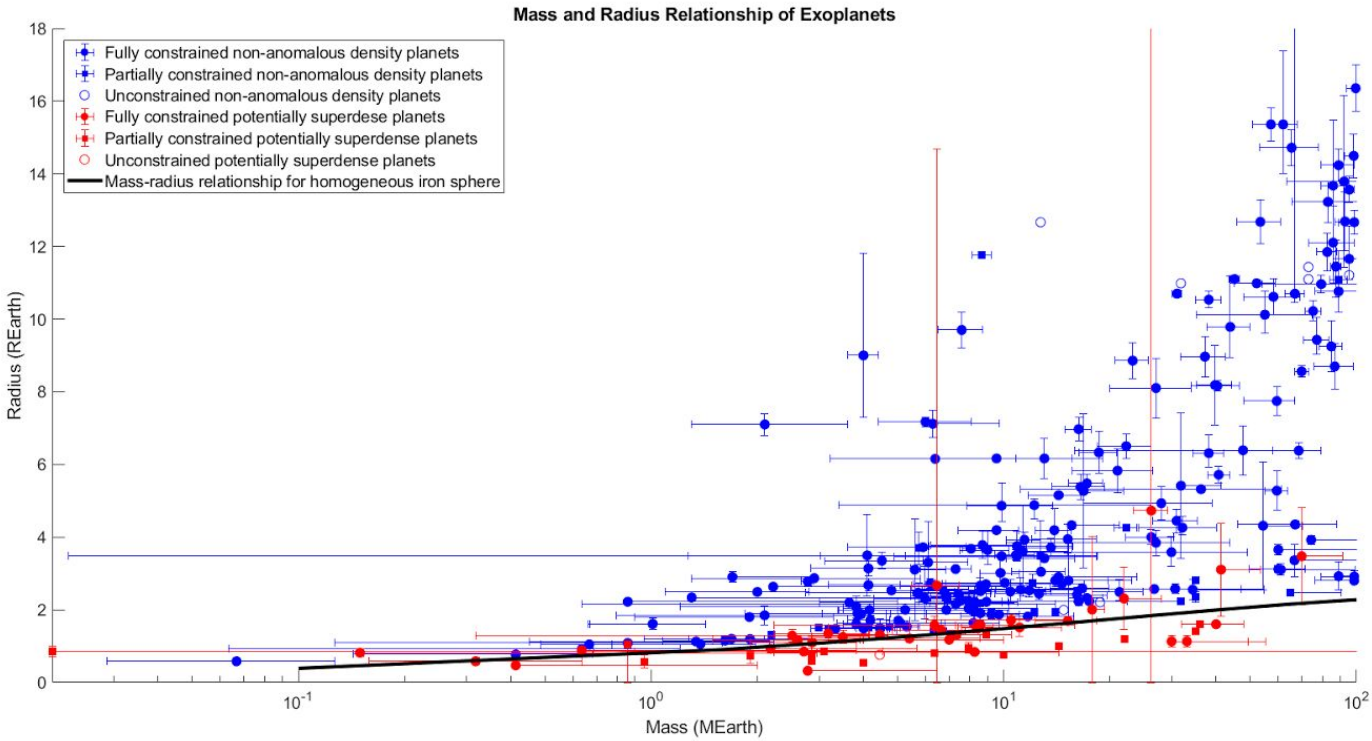

Fig 1 Mass vs radius for 236 planetary core candidates

Shown is the mass and radius (scaled by the Earth's mass and radius) of 236 viable planets, highlighting the division between planets with radii potentially smaller than that of an iron sphere of the same mass (red), and those that have larger radii (blue). This division corresponds to planets less dense than iron and more dense than iron, respectively. The black line at the bottom of the figure represents the mass-radius relationship for a hypothetical pure iron case. Points marked with a filled circle have published uncertainty for both mass and radius measurements, square points have published uncertainty only for a single axis, and hollow circles have no published uncertainty.

Those planets marked in blue in the Fig. 1 were then discarded and no longer considered, as they were less dense than iron and were not suitable as planetary core candidates. Most intriguing were those planets that lie significantly below the iron mass-radius line, as they imply additional mechanisms at work to significantly increase density. Focusing on the superdense planets, all points with the centroids of the rectangle bounded by their published uncertainty (or the center of the uncertainty line, in the case where uncertainty for only one dimension was published) near or above the iron mass-radius line were

additionally discarded, leaving only those points significantly below the iron mass-radius line. Figure 2 shows the remaining 24 superdense exposed core candidates.

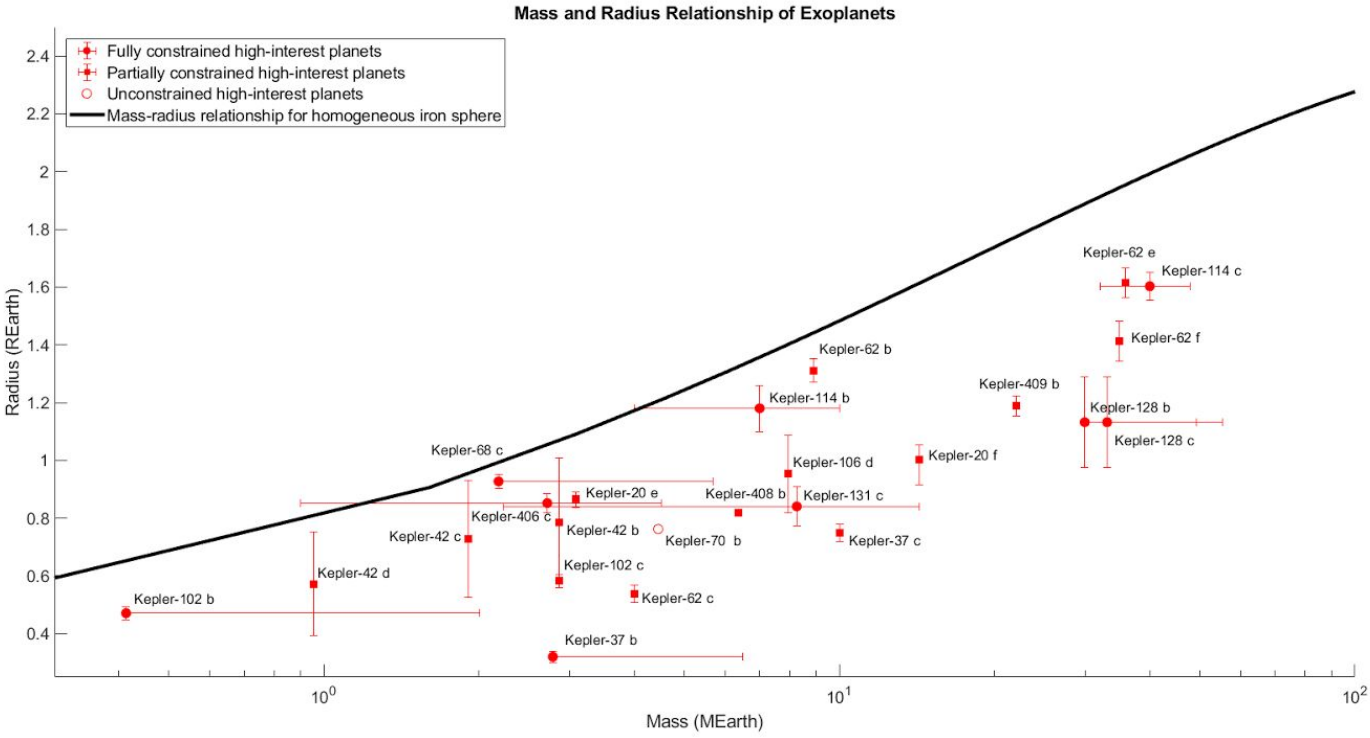

Fig 2. Mass vs radius for 24 superdense exoplanet core candidates

Mass and radius (scaled by the Earth's mass and radius) for high-interest potentially superdense candidates. Only points that were statistically likely to lay beneath the pure iron case (shown in black) were included. The points marked with filled circles are those that have published uncertainty for both mass and radius, square points have published uncertainty for only one axis, and those marked with an empty circle are those with no published uncertainty. The names of the planets are adjacent to their respective points.

The remaining 24 planets that lie below the pure iron case are of particular interest, as current models of planetary formation and evolution don't account for their existence. Barring incorrectly reported values or error in data processing by initial publishers, these candidates imply a particularly extraordinary history. Mocquet et al. (*7*) also investigated superdense planets of this very nature, identifying ten potentially

superdense candidates and focusing analysis on three well-defined examples (Kepler-52b, Kepler-52c and Kepler-57b) (*7*). However, the three planets analyzed in Mocquet et al. (*7*) were not identified as anomalous in this study, and have had conflicting data reported since the publication of the initial work. Additionally, 16 of the candidates found in this study had new data reported or updated after Mocquet et al. (*7*) was published, so the many potentially new candidates discovered here are particularly of interest.

Mocquet et al. (*7*) proposed a mechanism for the formation and evolution of these superdense planets, known as the "Fossilized Core Theory". Since the discovery of so-called 'Hot Jupiters', or massive giant planets exceedingly close to their host stars, planetary migration and rapid hydrodynamic escape has been studied in depth (*4-7, 14-19*). In situ formation of such large, gaseous bodies is incompatible with nearly every existing planetary formation model, so many proposed mechanisms have since been developed to explain their observed positions (*18, 19*). For the remainder of this study we will assume that these gas giants did indeed form far from their observed positions and migrated. The large gas giants indicative of Hot Jupiters that are the proposed primordial states of these superdense candidates have notably high central pressures (*20, 21*), enough to compress the cores to the observed densities of the anomalous planets. The Fossilized Core Theory suggests that some of these large migrating giant planets may have come too close to their host stars, and the increased thermal energy facilitated the loss of the majority of their atmospheres, leaving behind the noted superdense Chthonian "fossilized" cores. Once the gas envelope has eroded, the cores are left to slowly decompress back to traditional expected densities, and are in fact nearly indistinguishable from terrestrial planets (*7*). Two parameters are particularly important in assessing the validity of this theory: the atmospheric escape timescale and the core relaxation timescale. Mocquet et al. (*7*) demonstrated that under realistic but extreme circumstances, the atmospheric escape timescale can be several orders of magnitude smaller than the core relaxation timescale, an explanation of which is summarized here.

The escape method of the eroding planetary envelope may be dominated by one of three processes depending on the spacial, thermal, and compositional variations in the star, orbit, and planetary atmosphere. The three processes are either energy-limited escape, diffusion-limited escape or through blow-off (*22*). Valencia et al. (*21*) applied the extreme case of energy limited escape (where the atmospheric loss is proportional to the corrected ratio between the flux of the stellar ultraviolet radiation and the gravitational potential of the planet) to CoRot-7 b and found an atmospheric loss rate of 10^8 kg s^{-1} (*21*). This is supported by the 10^2 - 10^9 kg s^{-1} range hypothesized by Lecavelier des Etangs (*23*). Valencia et al. (*21*) proposed that a hydrogen-helium atmosphere would escape in 1Myr, while a water atmosphere would escape in closer to 1Gyr.

Mocquet et al. (*7*) calculated the time-varying evolution of the volumetric strain experienced by the planetary core during and after atmospheric escape, assuming stellar abundances of elements. Their results imply that for extremely high pressures, the unloading stress on the core can drastically affect the temporal evolution of the strain, in some situations even leading to a lost of cohesion of the planet if the atmospheric loss rate is significantly high (*7*). Their results suggest that for large planetary cores, the relaxation timescales may be several billions of years after atmospheric loss, making it plausible that the naked cores could be observed from Earth today, though their results do not take into account the rheological stratification of the planet, which could lead to further brittle deformations in the uppermost high-viscosity layers of the planet (*7*). Moving forward, we will assume that the Fossilized Core Theory describes the formation of superdense planets, and check the validity of the 24 core candidates identified here under the assumptions of this theory. The first requirement is that the proposed cores are consistent with the core accretion model or existing estimates for the core properties of solar system gas or ice giants.

The estimates for the planetary embryo properties necessary for runaway gas accretion under the core accretion model have conflicting conclusions (*24-25*). Some suggest that a core of 10-20M_{Earth} is required for gas giant formation (*24*), but in simulations, others are able to show that sufficiently large (100M_{Earth}) planets are able to form under relatively short timescales (~1Myr) with a small core of only 0.6M_{Earth} (*25*). Due to the conflicting results, for the scope of this study, we consider analyzing the existing estimates for the measured core properties of gas and ice giants in our own solar system to be more useful than debating the intricacies of the core accretion method, as we know that the gas giants in our solar system can and do exist with core masses as measured (albeit poorly constrained).

Uranus is thought to have an approximate core mass of 0.55M_{Earth} (*26*), Saturn is estimated to have a core mass of 9 - 22M_{Earth},(25, 27) and Jupiter is thought to have a core mass of between 12 and 45M_{Earth} (though in coming years the estimate is predicted to become more precise with new Juno data) (25, 27, 28). This study will be considering the upper ranges of Saturn and Jupiter's predicted core masses, as we are interested in the extremes of possibility. In addition, planets larger than Jupiter have been found (*29*) and its not unrealistic to speculate that they might have even greater core masses than the most extreme of estimates of Jupiter's core. Figure 3 shows again the 24 superdense fossilized Chthonian core candidates as well as the estimates for the solar system's giant planet's cores.

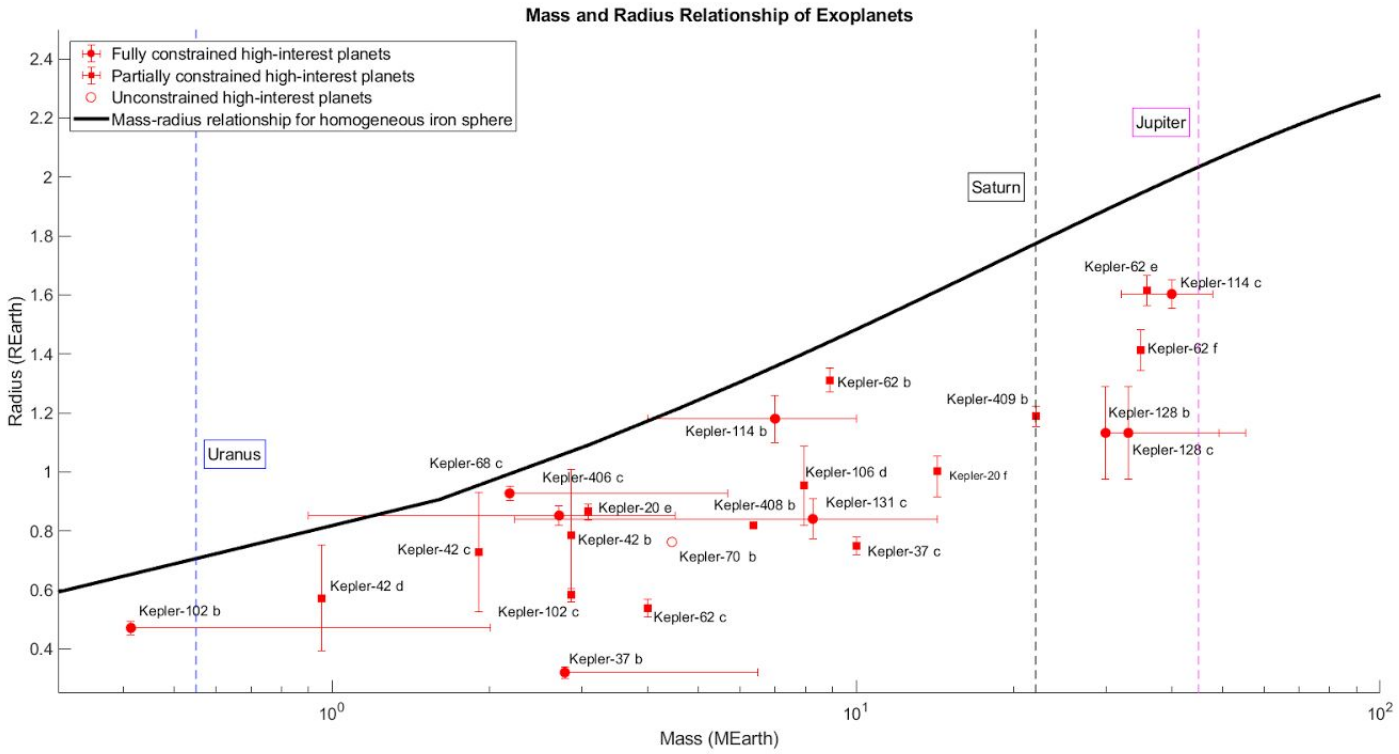

Fig. 3 A comparison of measured solar system core masses to the masses of proposed superdense fossilized cores The black line is the mass-radius case for a homogeneous sphere of pure iron. The red points are exoplanets that have measured data implying a density greater than that of an iron sphere of the same size. The points marked with a filled circle are those that have published uncertainties for both mass and radius, the filled squares are those that have published uncertainties for only one axis, and the empty circles are points that have no published uncertainties. The vertical dashed lines are the estimated core masses of (from right to left) Uranus, Saturn, and Jupiter. Note how all proposed candidates lie for the most part between the extremes.

The results of Fig. 3 are encouraging, as all candidates plausibly fit between the extremes of the proposed core masses of Uranus and Jupiter. This may imply that the low mass candidates had primordial envelopes consistent with that of Uranus or other ice giants, while the high mass cores had primordial envelopes more similar to very massive gas giants like Jupiter.

The second requirement is that the semimajor axis of the core candidates is consistent with that of Hot Jupiters. In order for the required rapid hydrodynamic escape processes to take place, there needs to be significant thermal contribution from the star. The expected semimajor axis range for Hot Jupiters is less than ~0.1 - 0.2AU (though Hot Jupiters detected through the radial velocity method tend to be biased towards semimajor axis around and greater than 0.5AU) (*30*). The Fossilized Core Theory relies on extreme conditions to explain the observed conditions, so we compared the published semimajor axis data to the most restrictive end of this scale at less than 0.2AU. Figure 4 illustrates this.

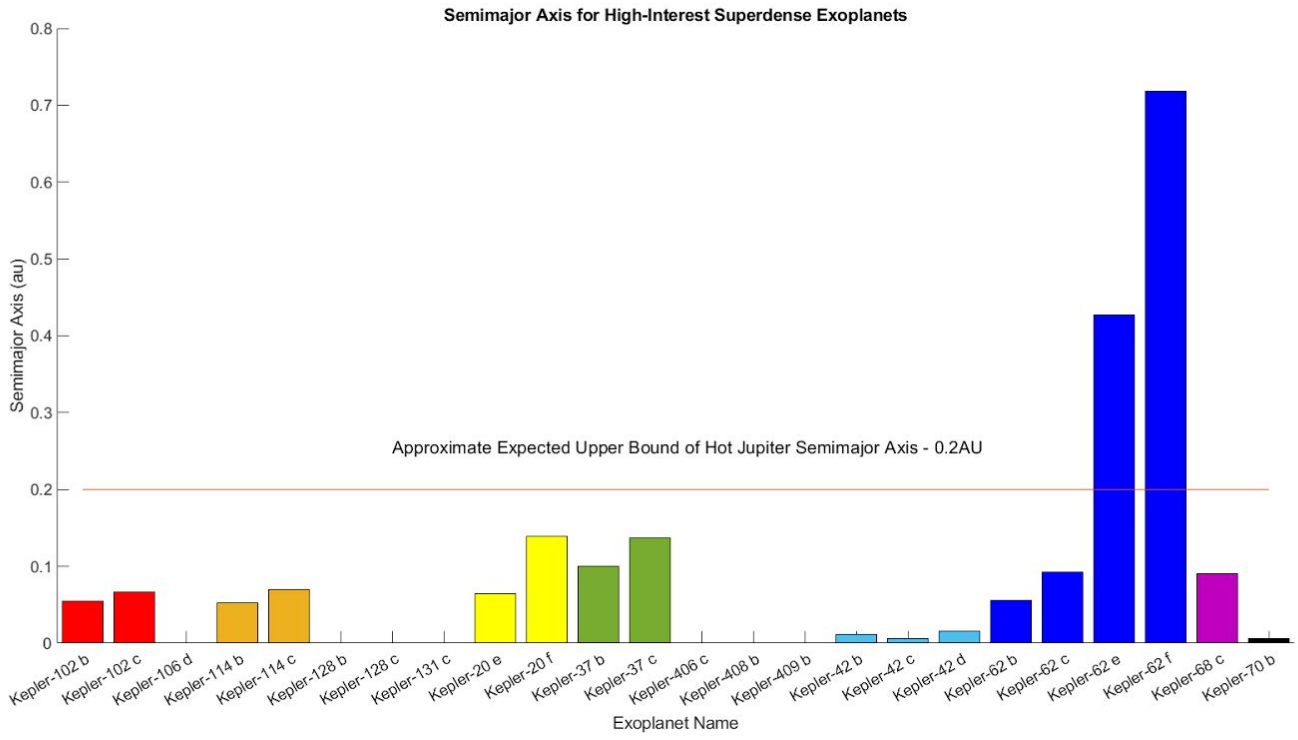

Fig. 4 Semimajor axis of superdense core candidates

This shows the published semimajor axis in astronomical units of all 24 planet candidates. Those with no bars do not have published semimajor axis data. The orange horizontal line marks a conservative upper limit for the semimajor axes of Hot Jupiters. The color of the bars corresponds to separate planetary systems, so while there are 24 planets, they represent only 14 unique planetary systems.

From Fig. 3 it can be seen that the majority of those planets with published semimajor axis data have semimajor axes significantly below 0.2AU, so are consistent with the proposed Fossilized Core Theory. The notable counterexamples are Kepler-62 e and Kepler-62 f, which have semimajor axes over twice as large as required by the limitations of this proposed mechanism. However, curiously, the Kepler 62 system is entirely anomalously dense planets. This may point to a systematic error in the analysis of the data, but as other systems consistent with the theory are shown to share the same anomalous density between planets, it may perhaps imply something about the formation of these planets and the structure of the early solar systems. Perhaps the Kepler-62 protoplanetary disk was especially well suited to migration, and all of the observed planets are indeed superdense Chthonian remnants. As there are four, orbital tides may have forced planets to migrate outwards again after losing substantial mass, as the inner solar system was too crowded to support so many planets. This is not the first example of all planets in a system sharing a density anomaly, as is the case with Kepler-11 having six surprisingly low density planets (*31*), so may be plausible. Similarly, while the range for Hot Jupiter semimajor axes was constrained to 0.2AU, specimens have been observed at distances of over 0.5AU, and depending on the temperature and flux of the star, could still get the required thermal energy to undergo rapid hydrodynamic escape.

While these results are encouraging, it should still be noted that many of the candidates have poorly constrained or unconstrained masses, so it's very possible that followup data in coming years will disqualify some of these candidates as potential superdense cores. Similarly, as the semimajor axis data is published for a larger set of the proposed cores, we may find that they are too far away from their stars to have undergone the proposed rapid envelope escape, in which case other mechanisms will need to be explored. However, as of this study, all 24 of the potential superdense planets show significant evidence of being consistent with the Fossilized Core Theory.

References and Notes:

1. J. D. Kendall, H. J. Melosh, Differentiated Planetesimal Impacts Into a Terrestrial Magma Ocean: Fate of the Iron Core. *Earth and Planetary Science Letters* **448**, 24-33 (2016).
2. K. Righter, D. P. O'Brein, Terrestrial Planet Formation. *PNAS* **108**, 19165-19170 (2011).
3. L. T. Elkins-Tanton *et al.*, Journey to a Metal World: Concept for a Discovery Mission to Psyche *45th Lunar and Planetary Science Conference* (2014).
4. D. Catling, K. Zahnle, The Escape of Planetary Atmospheres. *Scientific American*, (2009).
5. D. Ehrenreich *et al.*, Hubble sees Atmosphere Being Stripped From Neptune-Sized Exoplanet. *Nature* **522**, 459 – 461 (2015).
6. G. Hébrard, A. Lecavelier Des Etangs, A. Vidal-Madjar, J. M. D ésert, R. Ferlet, Evaporation Rate of Hot Jupiters and Formation of Chthonian Planets. *Extrasolar Planets: Today and Tomorrow, ASP Conference Proceedings* **321**, (2004).
7. A. Mocquet, O. Grasset, C. Sotin, Very High-Density Planets: A Possible Remnant of Gas Giants. *The Royal Society* **372**, (2014).
8. S. Seager, M. Kuchner, C. Heir-Majumder, B. Militzer, MASS-RADIUS RELATIONSHIPS FOR SOLID EXOPLANETS. *The Astrophysical Journal* **669**, (2007).
9. D. C. Swift *et al.*, Mass-Radius Relationships for Exoplanets. *The Astrophysical Journal* **744**, (2012).
10. L. Zeng, D. Sasselov, S. Jacobsen, Mass-Radius Relation for Rocky Planets Based on PREM. *The Astrophysical Journal* **819**, (2016).
11. L. Zeng, S. Jacobsen, A Simple Analytical Model for Rocky Planet Interiors. *The Astrophysical Journal* **837**, (2017).
12. S. E. Woosley, W. D. Arnett, D. D. Clayton, The Explosive Burning of Oxygen and Silicon. *Astrophysical Journal Supplement* **26**, (1973).

13. J. Schneider, C. Dedieu, P. Sidaner, R. Savalle, I. Zolotukhin, Defining and Cataloging Exoplanets: the exoplanet.eu database *Astronomy and Astrophysics* **532**, (2011).
14. N. V. Erkaev *et al.*, Roche Lobe Effects on the Atmospheric Loss from "Hot Jupiters". *Astronomy and Astrophysics* **472**, 329 - 334 (2007).
15. F. Tian, O. Toon, A. Pavlov, H. D. Sterck, Transonic Hydrodynamic Escape of Hydrogen from Extrasolar Planetary Atmospheres. *The Astrophysical Journal* **621**, (2004).
16. D. Valencia, M. Ikoma, T. Guillot, N. Nettelmann, Composition and Fate of Short-Period Super Earths - The Case of CoRot -7 b. *Astronomy and Astrophysics* **516**, (2010).
17. R. Yelle, H. Lammer, W.-H. Ip, Aeronomy of Extra-Solar Giant Planets *Space Science Reviews* **139**, 437–451 (2008).
18. A. Morbidelli, Scenarios of Giant Planet Formation and Evolution and Their Impact on the Formation of Habitable Terrestrial Planets *The Royal Society*, (2014).
19. R. P. Nelson, P. Hellary, S. M. Fendyke, G. Coleman, Planetary System Formation in Thermally Evolving Viscous Protoplanetary Discs *The Royal Society*, (2014).
20. D. Saumon, T. Guillot, Shock Compression of Deuterium and the Interiors of Jupiter and Saturn. *The Astrophysical Journal* **609**, 1170-1180 (2004).
21. D. Valencia, M. Ikoma, T. Guillot, N. Nettelmann, Composition and Fate of Short-Period Super Earths - The Case of CoRot -7 b. *Astronomy and Astrophysics* **516**, (2010).
22. F. Tian, J. F. Kasting, H.-L. Liu, R. G. Roble, Hydrodynamic Planetary Thermosphere Model: 1. Response of the Earth's Thermosphere to Extreme Solar EUV Conditions and the Significance of Adiabatic Cooling. *Journal of Geophysical Research* **113**, (2008).

23. A. Lecavelier des Etangs, A Diagram to Determine the Evaporation Status of Extrasolar Planets. *Astronomy and Astrophysics* **461**, 1185 - 1193 (2007).
24. C. Mordasini, Y. Alibert, W. Benz, D. Naef, Giant Planet Formation by Core Accretion. *Extreme Solar Systems, ASP Conference Series* **398**, (2008).
25. W. K. M. Rice, P. J. Armitage, On the Formation Timescale and Core Masses of Gas Giant Planets *The Astrophysical Journal* **598**, L55-L58 (2003).
26. M. Podolak, A. Weizman, M. Marley, Comparative Models of Uranus and Neptune. *Planetary and Space Science* **43**, 1517-1522 (1995).
27. D. Saumon, T. Guillot, Shock Compression of Deuterium and the Interiors of Jupiter and Saturn. *The Astrophysical Journal* **609**, 1170-1180 (2004).
28. T. Guillot, D. Gautier, W. B. Hubbard, New Constraints on the Composition of Jupiter from Galileo Measurements and Interior Models *Icarus* **30**, 534-539 (1997).
29. K. L. Luhman, T. L. Esplin, N. P. Loutrel, A Census of Young Stars and Brown Dwarfs in IC 348 and NGC 1333. *The Astrophysical Journal* **827**, (2016).
30. T. Currie, On the Semimajor Axis Distribution of Extrasolar Gas Giant Planets: Why Hot Jupiters Are Rare Around High-Mass Stars. *The Astrophysical Journal Letters* **694**, L171-L176 (2009).
31. J. Lissauer *et al.*, All Six Planets Known to Orbit Kepler-11 Have Low Density. *The Astrophysical Journal* **770**, (2013).

Acknowledgements:

A heartfelt thanks to the department of Earth, Atmospheric and Planetary Science for supporting this work, along with Benjamin P. Weiss and John Brooks Biersteker for their support and helpful guidance.

This gratitude extends to the entire 12.420 Essentials of Planetary Science class for being a supportive, positive, and encouraging learning and discussion environment.